

# Monitoring Hierarchical Assembly of Ring-in-Ring and Russian Doll Complexes Based on Carbon Nanoring by Förster Resonance Energy Transfer

Shengzhu Guo, Lin Liu, Feng Su, Huiji Yang, Guoqin Liu, Yanqing Fan, Jing He, Zhe Lian, Xiaonan Li, Weijie Guo, Xuebo Chen, and Hua Jiang\*



Cite This: *JACS Au* 2024, 4, 402–410



Read Online

ACCESS |

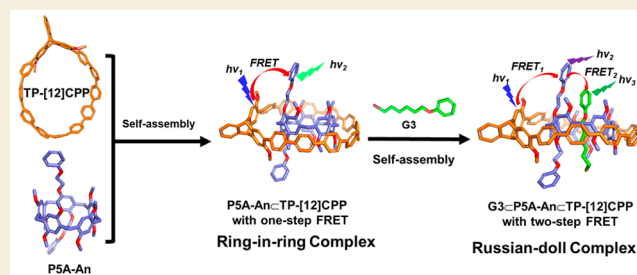
Metrics & More

Article Recommendations

Supporting Information

**ABSTRACT:** We presented the construction of the ring-in-ring and Russian doll complexes on the basis of triptycene-derived carbon nanoring (TP-[12]CPP), which not only acts as a host for pillar[5]arene (PSA) but also serves as an energy donor for building Förster resonance energy transfer (FRET) systems. We also demonstrated that their hierarchical assembly processes could be efficiently monitored in real time using FRET. NMR, UV–vis and fluorescence, and mass spectroscopy analyses confirmed the successful encapsulation of the guests PSA/PSA-An by TP-[12]CPP, facilitated by C–H⋯π and ⋯π interactions, resulting in the formation of a distinct ring-in-ring complex with a binding constant of  $K_a = 2.23 \times 10^4 \text{ M}^{-1}$ . The encapsulated PSA/PSA-An can further reverse its role to be a host for binding energy acceptors to form Russian doll complexes, as evidenced by the occurrence of FRET and mass spectroscopy analyses. The apparent binding constant of the Russian doll complexes was up to  $3.6 \times 10^4 \text{ M}^{-1}$ , thereby suggesting an enhanced synergistic effect. Importantly, the Russian doll complexes exhibited both intriguing one-step and sequential FRET dependent on the subcomponent PSA/PSA-An during hierarchical assembly, reminiscent of the structure and energy transfer of the light-harvesting system presented in purple bacteria.

**KEYWORDS:** Triptycene, Carbon nanohoop, Host–guest interaction, Russian doll complexes, FRET



## INTRODUCTION

The construction of novel supramolecular complexes with unique structures remains an intriguing but challenging objective in supramolecular chemistry.<sup>1,2</sup> Over the past few decades, various macrocycles, including cucurbituril,<sup>3–6</sup> crown ethers,<sup>7–9</sup> and blue box,<sup>10,11</sup> have been extensively utilized to fabricate impressive hierarchical assembled structures. Among them, nonintertwined ring-in-ring or host-in-host assemblies through host–guest recognitions between two different macrocycles have garnered significant interest<sup>12–21</sup> and are promising for the development of new materials, including multicolor biological imaging reagents and information encryption.<sup>6,22</sup> In particular, some Russian doll (matryoshka) complexes<sup>17,23,24</sup> are able to mimic the structure of the natural photosynthetic antenna systems in purple bacteria in which the light-harvesting reaction center (LH1-RC) architecture absorbs sunlight and directs the excitation energy from LH2 to LH1 and subsequently transfers to the RC encapsulated within the LH1 ring.<sup>25</sup>

Recently, carbon nanohoops,<sup>11,26–29</sup> in particular, [*n*]-cycloparaphenylenes ([*n*]CPPs),<sup>30–42</sup> have attracted considerable research attention because of their ability to host π-conjugated molecules with a complementary convex surface,

such as fullerene or metallofullerene. Both theoretical calculations and experimental investigations have demonstrated that larger CPPs could nest ever smaller ones to form a ring-in-ring complex when the ring size difference of CPPs reaches five phenylene units,<sup>43–47</sup> which further promotes the constructions of Russian doll complexes consisting of two differently sized carbon nanorings and (metallo)fullerenes.<sup>44</sup> However, there are limited examples of utilizing the carbon nanoring for encapsulating nonaromatic guests because of a lack of efficient concave–convex interactions between aromatic hosts and nonaromatic guests.<sup>48,49</sup> For instance, Dumele et al. developed a Russian doll complex by encapsulating a complex of crown ether–metal ions in the confined cavities of a carbon nanoring based on [5]cyclo-pyrenylene.<sup>29</sup> Recently, we<sup>39</sup> successfully constructed chiral Russian doll complexes on the basis of a planar chiral [2.2]paracyclophane-based CPP

**Received:** November 17, 2023

**Revised:** January 15, 2024

**Accepted:** January 17, 2024

**Published:** January 22, 2024



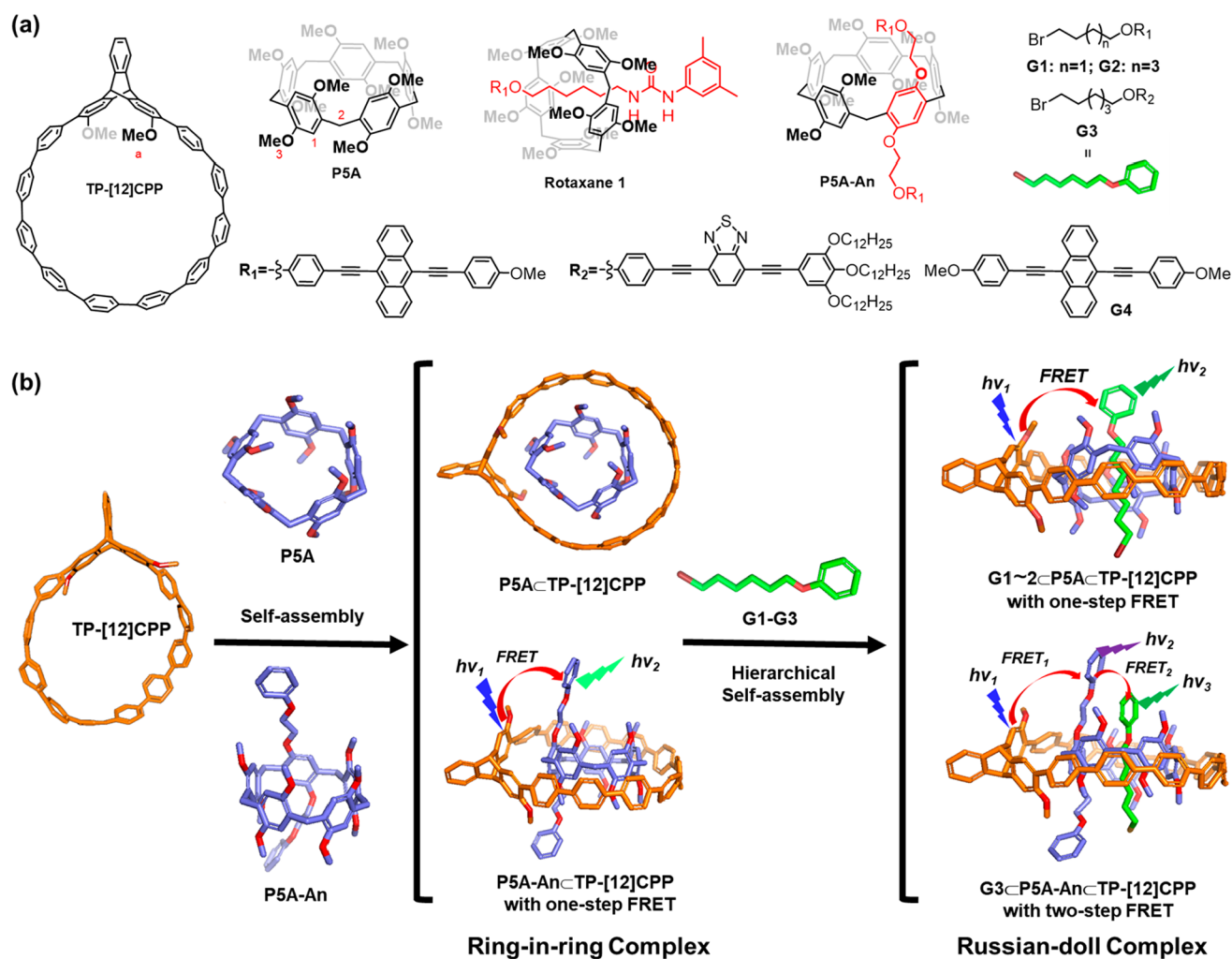


**Figure 1.** (a) The chemical structure of TP-[12]CPP, P5A, P5A-An, Rotaxane 1, and G1–G3. (b) The cartoon illustrations of FRET processes in the proposed ring-in-ring and Russian doll complexes in this work.

featuring highly selective chiral self-recognition for chiral amines. Nevertheless, Russian doll complexes based on carbon nanohoops are still very challenging to achieve.

The physicochemical methodologies, such as gel electrophoresis, atomic force microscopy, cryo-transmission electron microscopy, and X-ray analysis, are commonly employed for the characterization of supramolecular assemblies.<sup>50–52</sup> However, it is worth noting that these methodologies are often destructive and primarily allow for end-point analysis of the final product. This limitation hinders the ability to detect and optimize the assembly process through manipulation of the same sample.<sup>53</sup> Förster resonance energy transfer (FRET),<sup>54,55</sup> a nonradiative energy transfer process through dipole–dipole interaction between donor and acceptor, has been established as an ideal method for real-time monitoring of the processes and dynamics associated with supramolecular self-assembly,<sup>56–62</sup> which has widespread applications in fields like fluorescent probes,<sup>63,64</sup> chemosensors,<sup>65,66</sup> imaging agents,<sup>67–69</sup> photodynamic therapy,<sup>70,71</sup> and artificial light-harvesting systems (LHSs).<sup>72–75</sup> For instance, Rebek et al. successfully utilized FRET to characterize the dynamic features of supramolecular capsules on the basis of hydrogen bonds.<sup>56–58</sup> Yang presented the real-time monitoring of coordination-driven self-assembly dynamics through

FRET.<sup>59–62</sup> Recently, we have constructed two efficient FRET systems on the basis of heterotopic bisnanohoops<sup>41</sup> and double helicates<sup>74</sup> for achieving multiple color-tunable emissions, including white light LED devices, respectively.

More recently, we<sup>76</sup> reported the synthesis and properties of a novel series of nanometer-sized cavity triptycene (TP)-derived carbon nanohoops with highly fluorescence emission (the quantum yields achieved were up to 92.5%). Among these carbon nanohoops, TP-[12]CPP possesses a large cavity size (18.08 Å × 15.84 Å), as demonstrated in the solid phase, along with impressive (chir)optical properties. Encouraged by these observations, we anticipated that TP-[12]CPP would not only serve as a host for other macrocycles with corresponding dimensions so as to facilitate the formation of ring-in-ring complexes but could also act as an energy donor for FRET, which enables us to monitor the hierarchical assembly of supramolecular complexes via FRET. Notably, our theoretical calculations identified a striking similarity between the cavity of TP-[12]CPP and the contour of pillar[5]arene (P5A), which strongly suggests that TP-[12]CPP could potentially host P5A to form a ring-in-ring complex. Although it is well-known that P5A is mainly used as a host for encapsulating linear guests,<sup>77–83</sup> the utilization of P5A as a guest in the construction of nested supramolecular structures and, con-

sequently, for building Russian doll complexes via hierarchical assembly has been rarely documented.<sup>77–83</sup>

In this contribution, TP-[12]CPP, PSA, or its derivative PSA-An, was initially designed to construct ring-in-ring complexes, respectively. Linear, fluorescent guests G1–G3 were functionalized with different haloalkyl groups that are able to associate with PSA/PSA-An to form pseudo rotaxanes, which consequently form Russian doll complexes when encapsulated by TP-[12]CPP. The anthracene and benzothiazole derivatives were carefully chosen as fluorescent groups in G1–G3 to construct a FRET, which requires the excitation spectrum of the energy acceptor to be well overlapped with the emission spectrum of the energy donor (*vide infra*), so that the formation of ring-in-ring and Russian doll complexes could be monitored by FRET in real time. We demonstrated that the encapsulated PSA/PSA-An in ring-in-ring complexes showed a role reversal and became a host to bind linear guests (Figure 1b). Also, PSA-based Rotaxane 1 was prepared to form a Russian doll complex with TP-[12]CPP. As expected, a typical one-step FRET process was observed in the ring-in-ring complex of PSA-AnCTP-[12]CPP and the Russian doll complexes of G1–2CPSAAnCTP-[12]CPP and rotaxane 1CTP-[12]CPP. Notably, the Russian doll complexes of G3CPSA-AnCTP-[12]CPP displayed an intriguing sequential two-step FRET process reminiscent of the structure and energy transfer in typical purple bacteria.

## RESULTS AND DISCUSSION

### Construction of Ring-in-Ring Complex of PSACTP-[12]CPP

We first constructed ring-in-ring or Russian doll supramolecular structures by assembling TP-[12]CPP with PSA. <sup>1</sup>H NMR spectra revealed that the chemical shifts of protons in PSA showed an upfield shift upon addition of PSA into a solution of TP-[12]CPP in CDCl<sub>3</sub> (Figure 2a–c and Figures S6 and S7). For instance, protons H<sub>1</sub> and H<sub>3</sub> display obvious upfield shifts up to  $\Delta\delta = -0.04$  and  $-0.03$  ppm, respectively, which demonstrate that PSA experienced a shielded magnetic environment in the cavity of TP-[12]CPP and formed a ring-in-ring complex. Meanwhile, diffusion-ordered NMR spectroscopy (DOSY) experiments showed that the ring-in-ring complex PSACTP-[12]CPP displays one set of the distinct signal band for all components with a diffusion coefficient  $1.23 \times 10^{-9}$  m<sup>2</sup>/s [ $\log(D) = -8.91$ , Figure 2e and Figure S1], which is similar to that of free TP-[12]CPP [ $D = 1.44 \times 10^{-9}$  m<sup>2</sup>/s,  $\log(D) = -8.84$ , Figure 2d and Figure S2], thereby demonstrating a 1:1 stoichiometry of the nested complex PSACTP-[12]CPP in solution. Moreover, the 2D NOESY NMR spectrum of the 1:1 mixtures of PSA and TP-[12]CPP presented several obvious cross-peaks between TP-[12]CPP and PSA (Figure S4), which clearly confirmed the proximity of each component in the ring-in-ring complex and further provided solid evidence for the formation of a ring-in-ring complex. Moreover, the mass spectrum of the ring-in-ring complex PSACTP-[12]CPP was determined by ESI TOF-MS analysis, and the mass peak at  $m/z$  1845.7942 found for  $[M + Na]^+$  (Figure S49) further confirmed the formation of the ring-in-ring complex PSACTP-[12]CPP.

UV/vis absorption titration experiments (Figure S5a) revealed an increasing absorption at 295 nm and a decreasing one at 334 nm upon adding PSA to the TP-[12]CPP solution. Job's plots based on UV/vis spectra validated a 1:1 host–guest binding model (Figure S5b) with the binding constant of  $2.2 \times$

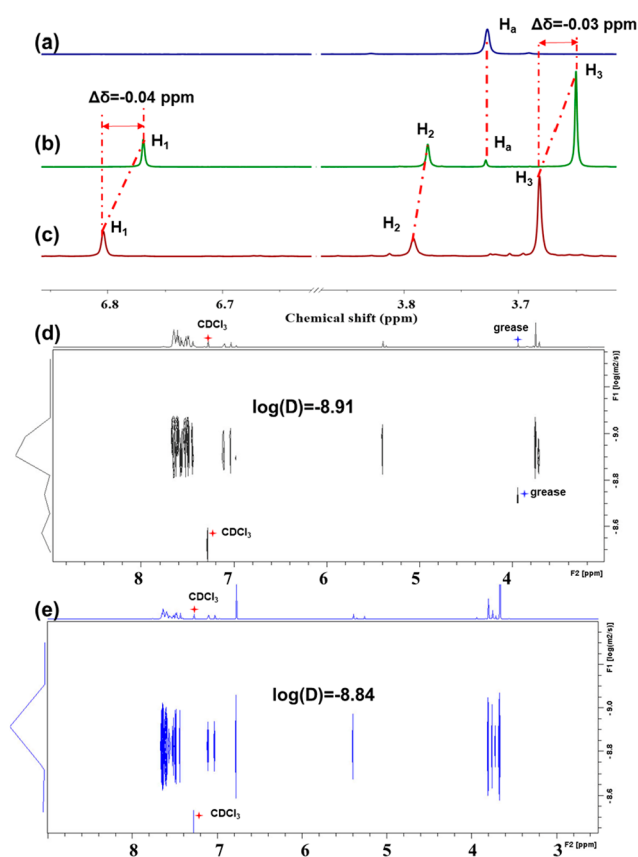


**Figure 2.** Partial <sup>1</sup>H NMR (600 MHz, 5 mM in CDCl<sub>3</sub>, 298 K) of (a) TP-[12]CPP, (b) PSACTP-12CPP (1:1), and (c) PSA. <sup>1</sup>H DOSY spectra (600 MHz, 5 mM in CDCl<sub>3</sub>, 298 K) of (d) TP-12CPP and (e) PSACTP-12CPP (1:1). The red plus sign is the signal of CDCl<sub>3</sub>, and the blue plus sign is the signal of grease.

$10^4$  M<sup>-1</sup> (Table 1), thereby suggesting a strong interaction between TP-[12]CPP and PSA. Moreover, an independent

**Table 1. Summary of Apparent Binding Constants  $K_a$  (M<sup>-1</sup>) and  $\Phi_{ET}$  Calculated of Different Complexes**

complexes	$K_a$ /M <sup>-1</sup> ( $\times 10^4$ ) <sup>d</sup>	$\Phi_{ET}$
PSACTP-[12]CPP	$2.2 \pm 0.1^a$	
G1CPSA	$(2.9 \pm 0.1) \times 10^{2b}$	
G1CPSACTP-[12]CPP	$3.5 \pm 0.1^c$	75%
G2CPSACTP-[12]CPP	$3.1 \pm 0.2^c$	61%
Rotaxane 1CTP-[12]CPP	$2.9 \pm 0.1^c$	48%
PSA-AnCTP-[12]CPP	$2.2 \pm 0.1^c$	80%
G3CPSA-AnCTP-[12]CPP	$3.3 \pm 0.1^c$	95%
G3CPSA-An	$1.2 \pm 0.1^c$	43%

<sup>a</sup>The results were determined by UV–vis titration experiments. <sup>b</sup>The results were determined by NMR titration experiments. <sup>c</sup>The results were determined by FL titration experiments. <sup>d</sup>The results were according to triplicate experiments.

gradient model based on Hirshfeld partition (IGMH) analysis<sup>84</sup> (Figure 3a) revealed the presences of both C–H $\cdots\pi$  and  $\pi\cdots\pi$  interactions in the PSACTP-[12]CPP complex, which played the crucial roles in the formation of a stable ring-in-ring complex.



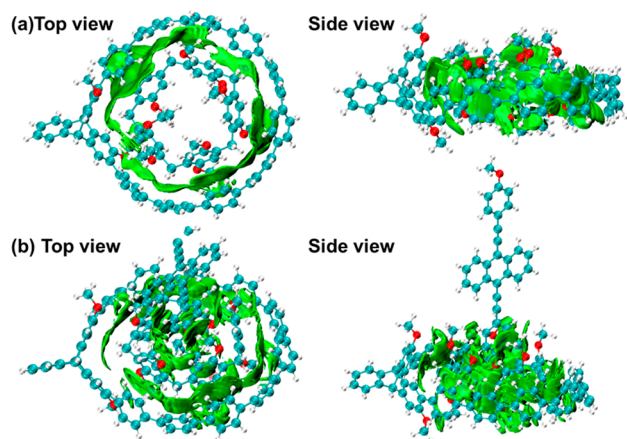


**Figure 3.** IGMH analyses of (a) the ring-in-ring complex of P5ACTP-12CPP and (b) the Russian doll complex of G1CP5ACTP-12CPP ( $\delta g_{\text{inter}} = 0.002$ ).

### Construction of Russian Doll Complexes on the Basis of P5ACTP-[12]CPP and G1–G2 with One-Step FRET

The encapsulation of PSA by TP-[12]CPP renders the central cavity of PSA available for binding a guest, which provides an appealing opportunity to construct Russian doll complexes. Therefore, two haloalkyl derivatives of 9,10-bis-(phenylethynyl)-anthracene, G1 and G2, whose excitation spectra (Figures S17, S18) overlap well with the emission of TP-[12]CPP, were selected as linear guests and energy acceptors for the construction of Russian doll complexes, which was monitored through FRET. The complexation of PSA with G1–G2 was confirmed through  $^1\text{H}$  NMR experiments (Figures S8–S10). For instance, the proton peaks of PSA exhibited downshifts upon addition of G1, presumably due to multiple C–H $\cdots\pi$  interactions between the curved surface of PSA and G1, which indicated the complexation between PSA and G1. Meanwhile, the binding constant  $K_a$  between PSA and G1 was estimated to be  $2.9 \times 10^2 \text{ M}^{-1}$  (Figure S9b). To further validate the hierarchical assembly of the ternary complex, we also carried out  $^1\text{H}$  NMR experiments (Figure 4b) by adding the complex of 1:1 G1CP5A into a solution of TP-[12]CPP. The results revealed the proton of PSA in the G1CP5ACTP-[12]CPP region exhibited upfield shifts with  $\Delta\delta = -0.07$  and  $-0.04$  ppm for H<sub>1</sub> and H<sub>3</sub>, respectively, which were attributed to the multiple C–H $\cdots\pi$  and  $\pi\cdots\pi$  interactions between PSA and TP-[12]CPP, as well as G1, thereby suggesting the successful formation of Russian doll complexes. Furthermore, the DOSY spectrum (Figure 4d) of the Russian doll complex G1CP5ACTP-[12]CPP also displayed a single-set signal band with a diffusion coefficient of  $3.47 \times 10^{-9} \text{ m}^2/\text{s}$  [ $\log(D) = -8.46$ ], which provided additional evidence for the formation of the Russian doll complexes. Independent gradient model based on Hirshfeld partition (IGMH) analysis (Figure 3b) unveiled that the long-chain alkane of G1 was effectively accommodated within the inner cavity of P5ACTP-[12]CPP, accompanied by multiple C–H $\cdots\pi$  and  $\cdots\pi$  interactions in stabilizing the Russian doll complexes.

Fluorescence titration experiments provided obvious evidence for the formation of the Russian doll complexes. When the G1CP5A complex (1:1) was titrated into TP-[12]CPP solution in chloroform (Figure 5a), an increase in the emission

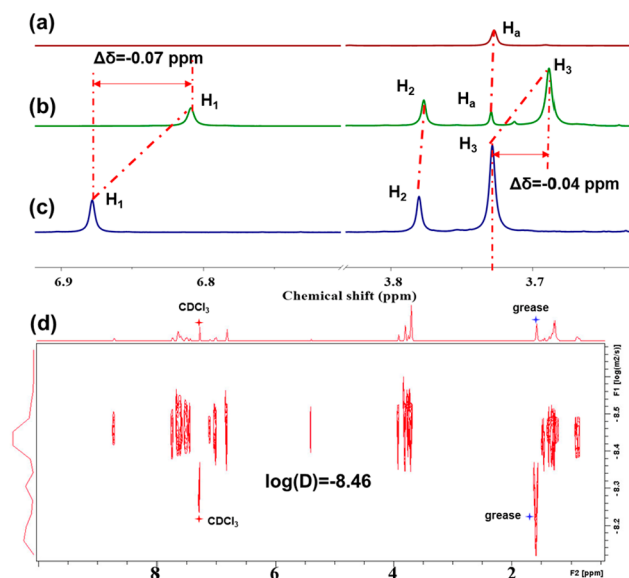


**Figure 4.** Partial  $^1\text{H}$  NMR (600 MHz, 5 mM in  $\text{CDCl}_3$ , 298 K) of (a) TP-[12]CPP, (b) G1CP5ACTP-12CPP (1:1:1), and (c) G1CP5A (1:1). (d)  $^1\text{H}$  DOSY spectra (600 MHz, 5 mM in  $\text{CDCl}_3$ , 298 K) of G1CP5ACTP-12CPP (1:1:1). The red plus sign is the signal of  $\text{CDCl}_3$ , and the blue plus sign is the signal of grease.

of G1 ( $\lambda_{\text{em}} = 493 \text{ nm}$ ) and a decrease in that of TP-[12]CPP ( $\lambda_{\text{em}} = 450 \text{ nm}$ ) were observed when excited at  $\lambda = 330 \text{ nm}$ . This behavior is indicative of the typical FRET process, which suggests that energy transfer occurs from TP-[12]CPP to G1 due to the formation of the Russian doll complexes. The apparent binding constant<sup>11,39</sup> of TP-[12]CPP for G1CP5A was estimated to be  $3.5 \times 10^4 \text{ M}^{-1}$  (Table 1 and Figure S22), which is obviously higher than that of TP-[12]CPP for PSA, thereby indicating that the presence of G1 enhances the binding affinity between TP-[12]CPP and PSA. This finding is consistent with that of the Russian dolls reported by Stoddart et al.<sup>11</sup> The efficiency of energy transfer ( $\Phi_{\text{ET}}$ ) was calculated to be 78% according to the previous reports (Table 1 and the Supporting Information).<sup>72,73</sup> Similar observations were found for the Russian doll complex of G2CP5ACTP-[12]CPP (Figure 5d–f and Table 1), which further confirmed the hierarchical self-assembly of Russian doll complexes that can be monitored through FRET. The mass peak at  $m/z$  2432.1001 was found for G2CP5ACTP-[12]CPP (Figure S50), which corresponded to the charge states of  $[\text{M} + \text{Na}]^+$ . In parallel, we synthesized a PSA-based Rotaxane 1 to create a Russian doll complex with TP-[12]CPP for comparing the binding abilities of TP-[12]CPP toward Rotaxane 1 and the pseudorotaxane G2CP5A. Fluorescence titration experiments (Figure S27) between TP-[12]CPP and Rotaxane 1 were conducted to confirm energy transfer taking place from TP-[12]CPP to Rotaxane 1 due to the formation of the Russian doll complexes. The binding constant of TP-[12]CPP for Rotaxane 1 was determined to be  $2.9 \times 10^4 \text{ M}^{-1}$ , which is comparable with that of TP-[12]CPP for pseudorotaxane G2CP5A, thereby suggesting that TP-[12]CPP possesses a comparable capacity for encapsulating both rotaxane and pseudo-one. The formation of Russian doll Rotaxane 1CTP-[12]CPP was further confirmed by HRMS with the mass peaks at  $m/z$  2494.3232 and 2517.2683 for  $[\text{M} + \text{H}]^+$  and  $[\text{M} + \text{Na}]^+$ , respectively (Figure S51). Additionally, the average

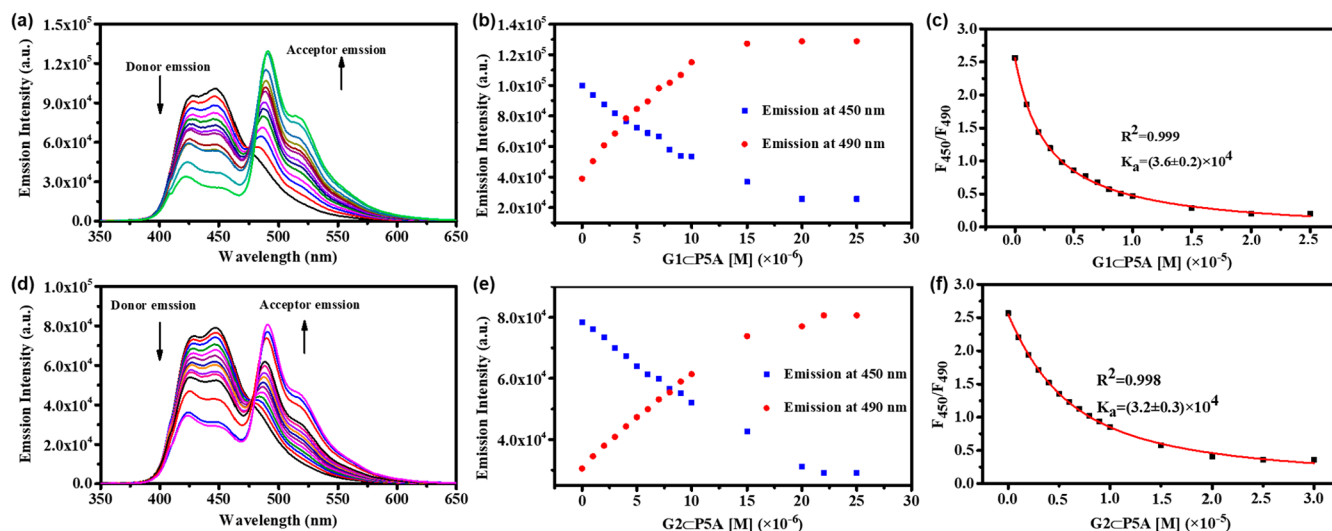


**Figure 5.** Fluorescence emission spectra of TP-[12]CPP ( $1 \times 10^{-5}$  M,  $\lambda_{\text{ex}} = 330$  nm) titrated with (a) G1CPSA ( $1 \times 10^{-3}$  M/ $1 \times 10^{-3}$  M) and (d) G2CPSA ( $1 \times 10^{-3}$  M/ $1 \times 10^{-3}$  M). Fluorescent intensity changes at 450 and 490 nm when titrated with (b) G1CPSA and (e) G2CPSA. Fluorescence emission titration plot for determination of the binding constant of TP-[12]CPP in the presence of (c) G1CPSA and (f) G2CPSA.

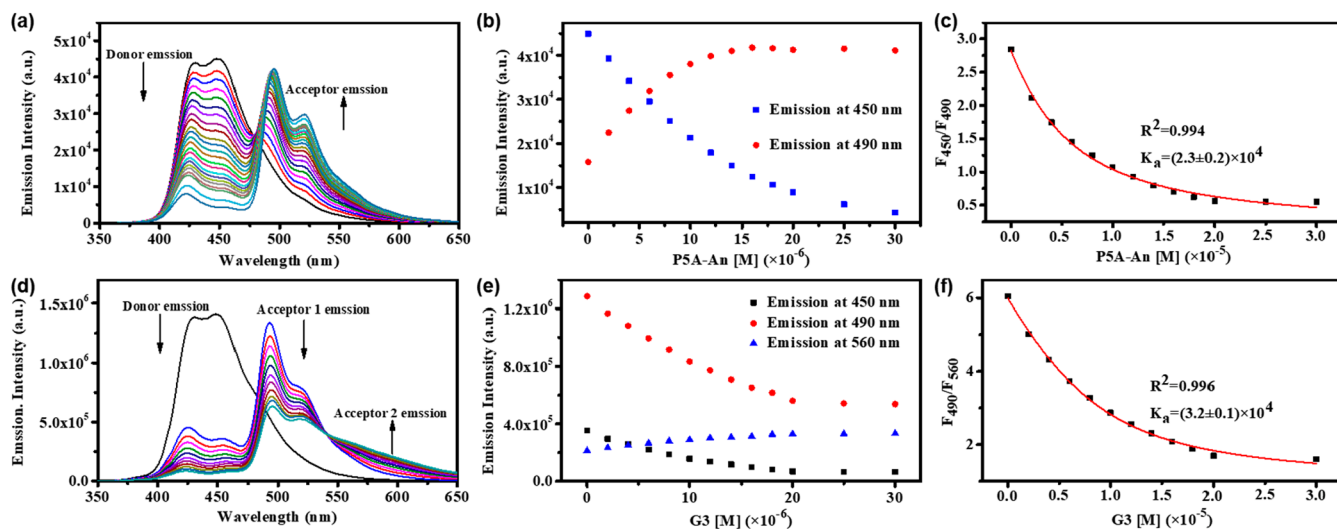


**Figure 6.** Fluorescence emission spectra of (a) TP-[12]CPP ( $1 \times 10^{-5}$  M,  $\lambda_{\text{ex}} = 330$  nm) titrated with P5A-An ( $1 \times 10^{-3}$  M) and (d) P5A-AnCTP-[12]CPP ( $2 \times 10^{-5}$  M/ $1 \times 10^{-5}$  M) titrated with G3 ( $1 \times 10^{-3}$  M). Fluorescent intensity changes of (b) TP-[12]CPP titrated with P5A-An and (e) P5A-AnCTP-[12]CPP ( $2 \times 10^{-5}$  M/ $1 \times 10^{-5}$  M,  $\lambda_{\text{ex}} = 330$  nm) titrated with G3. Fluorescence emission titration plot for determination of the binding constant of (c) TP-[12]CPP in the presence of P5A-An and (f) P5A-AnCTP-[12]CPP in the presence of G3.

lifetime of TP-[12]CPP was measured to be 0.98 ns, which increased to 1.55 ns upon the addition of P5A to TP-[12]CPP (Figures S34–S36 and Table S1). However, the addition of G1 and G2 into P5ACTP-[12]CPP resulted in a decrease in the average lifetime to 1.47 ns, which further supported the occurrence of FRET energy transfer from TP-[12]CPP to G1 and G2. Furthermore, a control experiment carried out by gradual addition of the mixture of P5A and G4 (1:1) into a solution of TP-[12]CPP (Figure S26) revealed no FRET takes place. This phenomenon strongly implies that the haloalkyl chains are indispensable for host–guest interactions between P5A/P5A-An and G1–G3.

#### Construction of Russian Doll Complexes on the Basis of P5A-AnCTP-[12]CPP and G3 with Sequential FRET

Finally, we attempted to fabricate a two-step energy transfer system, which is widely found in LHSs responsible for

capturing solar energy vital to living organisms.<sup>25,67–69</sup> To construct a Russian doll complex with a two-step FRET process, we rationally introduced 9,10-bis(phenylethynyl)anthracene to P5A to create P5A-An as an energy acceptor whose excitation spectrum overlapped with the emission spectrum of TP-[12]CPP (Figure S20). <sup>1</sup>H NMR experiments demonstrated that TP-[12]CPP is able to bind P5A-An, thus forming a ring-in-ring complex (Figures S14 and S15). Also, the formation of P5A-AnCTP-[12]CPP was confirmed by HRMS measurement (Figure S52), which shows the mass peak at  $m/z = 2718.2947$  for  $[M + \text{Na}]^+$ . Furthermore, fluorescence titration experiments demonstrated that the emission intensity of TP-[12]CPP decreased at 450 nm, while the emission intensity of P5A-An increased at 493 nm upon titration of 0–2 equiv of P5A-An (Figure 6a). The binding constant of TP-[12]CPP for P5A-An was estimated to

be  $2.2 \times 10^4 \text{ M}^{-1}$  (Table 1), which is consistent with that of TP-[12]CPP for the pristine P5A, and the  $\Phi_{\text{ET}}$  was calculated to be 80% (Table 1).

In order to construct a Russian doll complex with two-step energy transfer processes, benzothiadiazole derivative G3, whose excitation spectrum overlaps well with the emission of P5A-An (Figure S20), was selected as a guest and energy acceptor for the P5A-AnCTP-[12]CPP complex. We initially validated the host-guest complexation between P5A-An and G3 through fluorescence titrations (Figure S18). The results revealed that P5A-An effectively served as a host for G3 with a binding constant of  $1.1 \times 10^4 \text{ M}^{-1}$ . Therefore, G3 was titrated into the above P5A-AnCTP-[12]CPP binary complex for constructing G3CP5A-AnCTP-[12]CPP. Intriguingly, the fluorescence emission of TP-[12]CPP and P5A-An decreases significantly, while that of G3 increases around 550–650 nm upon titration of G3 (Figure 6d). The  $\Phi_{\text{ET}}$  was calculated to be 95% (Table 1). Meanwhile the average lifetimes of the ring-in-ring complex P5A-AnCTP-[12]CPP and the Russian doll complex G3CP5A-AnCTP-[12]CPP were measured to be 1.96 and 1.94 ns, respectively (Figures S37 and S38). These results clearly demonstrated that Russian doll complex G3CP5A-AnCTP-[12]CPP with two-step sequential energy transfer was effectively constructed.<sup>73,74</sup> The apparent binding constant of P5A-AnCTP-[12]CPP for binding G3 was determined to be  $3.1 \times 10^4 \text{ M}^{-1}$  (Table 1 and Figure S33), which is larger than that of P5A-An for binding G3, as well as that of TP-[12]CPP for P5A-An, thereby indicating a strong synergistic effect in the Russian doll complex. To shed light on the host-guest interactions between the complexes, the energies of the binary and ternary complexes were calculated and are presented in Table S2. The results indicated that the energies of Russian dolls are much lower than those of binary complexes, thereby suggesting that Russian dolls are more stable than binary complexes, which is indicative of the synergistic effect.<sup>85</sup> These observations suggest that our Russian doll could mimic the structure of the natural photosynthetic antenna systems and transfer energy, as observed in typical purple bacteria.<sup>17</sup> Specifically, the Russian doll complexes absorb sunlight and direct the excitation energy from TP-[12]CPP to P5A-An, which subsequently funnels to G3 encapsulated within P5A-An (Figure 2b).

## CONCLUSION

In summary, we demonstrated that TP-[12]CPP not only accommodates P5A or its derivatives P5A-An but also effectively encapsulate their complexes with linear guests in their open concave cavity to form a novel ring-in-ring complex and Russian doll complexes, respectively. We further presented that TP-[12]CPP can be used as an energy donor for constructing one-step and sequential FRET systems. The fluorescence titration experiments confirmed the occurrences of FRET during the formation of these ring-in-ring and Russian doll complexes, thereby indicating that the assembly process could be monitored using FRET. Notably, the Russian doll complex of G3CP5A-AnCTP-[12]CPP displayed a sequential energy transfer process that could mimic the structure and energy transfer in typical purple bacteria. These results not only emphasize the effectiveness of matching the dimensions of two distinct macrocycles for the development of hybrid supramolecular assemblies involving ring-in-ring complexes and smaller neutral guest molecules but also

illustrate the value of FRET as a powerful tool for monitoring the formation of binary or Russian doll complexes.

## ASSOCIATED CONTENT

### Supporting Information

The Supporting Information is available free of charge at <https://pubs.acs.org/doi/10.1021/jacsau.3c00720>.

Experimental details, additional NMR, mass spectroscopy, and fluorescence titration experiments (PDF)

## AUTHOR INFORMATION

### Corresponding Author

Hua Jiang – College of Chemistry, Beijing Normal University, Beijing 100875, P.R. China; [orcid.org/0000-0002-9917-2683](https://orcid.org/0000-0002-9917-2683); Email: [jiangh@bnu.edu.cn](mailto:jiangh@bnu.edu.cn)

### Authors

Shengzhu Guo – College of Chemistry, Beijing Normal University, Beijing 100875, P.R. China

Lin Liu – College of Chemistry, Beijing Normal University, Beijing 100875, P.R. China

Feng Su – College of Chemistry and Environmental Engineering, Shenzhen University, Shenzhen, Guangdong 518060, P.R. China

Huiji Yang – College of Chemistry, Beijing Normal University, Beijing 100875, P.R. China

Guoqin Liu – College of Chemistry, Beijing Normal University, Beijing 100875, P.R. China

Yanqing Fan – College of Chemistry, Beijing Normal University, Beijing 100875, P.R. China

Jing He – College of Chemistry, Beijing Normal University, Beijing 100875, P.R. China

Zhe Lian – College of Chemistry, Beijing Normal University, Beijing 100875, P.R. China

Xiaonan Li – College of Chemistry, Beijing Normal University, Beijing 100875, P.R. China

Weijie Guo – College of Chemistry, Beijing Normal University, Beijing 100875, P.R. China

Xuebo Chen – College of Chemistry, Beijing Normal University, Beijing 100875, P.R. China; [orcid.org/0000-0002-9814-9908](https://orcid.org/0000-0002-9814-9908)

Complete contact information is available at: <https://pubs.acs.org/doi/10.1021/jacsau.3c00720>

### Author Contributions

CRedit: Shengzhu Guo conceptualization, data curation, formal analysis, investigation, methodology, software, writing-original draft, writing-review & editing; Lin Liu methodology, software; Huiji Yang investigation, methodology; Guoqin Liu methodology, software; Yanqing Fan data curation, software; Jing He data curation, formal analysis; Zhe Lian formal analysis, software; Xiaonan Li software; Weijie Guo investigation, methodology; Xuebo Chen methodology, software; Hua Jiang conceptualization, methodology, project administration, resources, supervision, writing-original draft, writing-review & editing.

### Notes

The authors declare no competing financial interest.



## ACKNOWLEDGMENTS

This work was financially supported by the National Natural Science Foundation of China (22271019 and 21971020) and Beijing Natural Science Foundation (2212008). We thank Dr. Aijiao Guan at Institute of Chemistry, Chinese Academy of Sciences, for assistance with 2D NMR measurements. We also thank Prof. Dr. Xiaopeng Li and Dr. Heng Wang at College of Chemistry and Environmental Engineering, Shenzhen University, for assistance with HRMS measurements.

## REFERENCES

- (1) Lehn, J. M. *Supramolecular Chemistry*; VCH Publishers: New York, 1995.
- (2) Steed, J. W.; Atwood, J. L. *Supramolecular Chemistry*; John Wiley & Sons Ltd: Chichester, England, 2009.
- (3) Kim, S.-Y.; Jung, I.-S.; Lee, E.; Kim, J.; Sakamoto, S.; Yamaguchi, K.; Kim, K. Macrocycles within Macrocycles: Cyclen, Cyclam, and Their Transition Metal Complexes Encapsulated in Cucurbit[8]uril. *Angew. Chem., Int. Ed.* **2001**, *40*, 2119–2121.
- (4) Day, A.; Blanch, R. J.; Arnold, A. P.; Lorenzo, S. G. R.; Lewis, Dance, I. A Cucurbituril-Based Gyroscane: A New Supramolecular Form. *Angew. Chem., Int. Ed.* **2002**, *41*, 275–277.
- (5) Gong, W.; Yang, X.; Zavalij, P. Y.; Isaacs, L.; Zhao, Z.; Liu, S. From Packed “Sandwich” to “Russian Doll”: Assembly by Charge-Transfer Interactions in Cucurbit[10]uril. *Chem.—Eur. J.* **2016**, *22*, 17612–17618.
- (6) Wu, H.; Wang, Y.; Jones, L. O.; Liu, W.; Song, B.; Cui, Y.; Cai, K.; Zhang, L.; Shen, D.; Chen, X.-Y.; Jiao, Y.; Stern, C. L.; Li, X.; Schatz, G. C.; Stoddart, J. F. Ring-in-Ring(s) Complexes Exhibiting Tunable Multicolor Photoluminescence. *J. Am. Chem. Soc.* **2020**, *142*, 16849–16860.
- (7) Parac, T. N.; Scherer, M.; Raymond, K. N. Host within a Host: Encapsulation of Alkali Ion-Crown Ether Complexes into a  $[\text{Ga}_4\text{L}_6]^{12-}$  Supramolecular Cluster. *Angew. Chem., Int. Ed.* **2000**, *39*, 1239–1242.
- (8) Dalgarno, S. J.; Atwood, J. L.; Raston, C. L. Sulfonatocalixarenes: molecular capsule and ‘Russian doll’ arrays to structures mimicking viral geometry. *Chem. Commun.* **2006**, *44*, 4567–4574.
- (9) Dalgarno, S. J.; Fisher, J.; Raston, C. L. Interplay of p-Sulfonatocalix[4]arene and Crown Ethers En Route to Molecular Capsules and “Russian Dolls”. *Chem.—Eur. J.* **2006**, *12*, 2772–2777.
- (10) Danjo, H.; Hashimoto, Y.; Kiden, Y.; Nogamine, A.; Katagiri, K.; Kawahata, M.; Miyazawa, T.; Yamaguchi, K. Nestable Tetraakis(spiroborate) Nanocycles. *Org. Lett.* **2015**, *17*, 2154–2157.
- (11) Cai, K.; Lipke, M. C.; Liu, Z.; Nelson, J.; Cheng, T.; Shi, Y.; Cheng, C.; Shen, D.; Han, J.-M.; Vemuri, S. I.; Feng, Y.; Stern, C. L.; Goddard, W. A.; Wasielewski, M. R.; Stoddart, J. F. Molecular Russian dolls. *Nat. Commun.* **2018**, *9*, 5275.
- (12) Chiu, S.-H.; Pease, A. R.; Stoddart, J. F.; White, A. J. P.; Williams, D. J. A Ring-in-Ring Complex. *Angew. Chem., Int. Ed.* **2002**, *41*, 270–274.
- (13) Forgan, R. S.; Friedman, D. C.; Stern, C. L.; Bruns, C. J.; Stoddart, J. F. Directed self-assembly of a ring-in-ring complex. *Chem. Commun.* **2010**, *46*, 5861–5863.
- (14) Forgan, R. S.; Wang, C.; Friedman, D. C.; Spruell, J. M.; Stern, C. L.; Sarjeant, A. A.; Cao, D.; Stoddart, J. F. Donor–Acceptor Ring-in-Ring Complexes. *Chem.—Eur. J.* **2012**, *18*, 202–212.
- (15) Klosterman, J. K.; Veliks, J.; Frantz, D. K.; Yasui, Y.; Loepfe, M.; Zysman-Colman, E.; Linden, A.; Siegel, J. S. Conformations of large macrocycles and ring-in-ring complexes. *Org. Chem. Front.* **2016**, *3*, 661–666.
- (16) Moorthy, J. N.; Natarajan, P. GuestCGuestCHost Multi-component Molecular Crystals: Entrapment of GuestCGuest in Honeycomb Networks Formed by Self-Assembly of 1,3,5-Tri(4-hydroxyaryl)benzenes. *Chem.—Eur. J.* **2010**, *16*, 7796–7802.
- (17) Rousseaux, S. A. L.; Gong, J. Q.; Haver, R.; Odell, B.; Claridge, T. D. W.; Herz, L. M.; Anderson, H. L. Self-Assembly of Russian Doll Concentric Porphyrin Nanorings. *J. Am. Chem. Soc.* **2015**, *137*, 12713–12718.
- (18) Lei, Z. Q.; Polen, S.; Hadad, C. M.; RajanBabu, T. V.; Badjić, J. D. Russian Nesting Doll Complexes of Molecular Baskets and Zinc Containing TPA Ligands. *J. Am. Chem. Soc.* **2016**, *138*, 8253–8258.
- (19) Han, Y.; Liang, T.-L.; Hao, X.; Chen, C.-F. Solid-state “Russian doll”-like capsules based on a triptycene-derived macrotricyclic host with paraquat derivative and polycyclic aromatic hydrocarbons. *CrystEngComm* **2016**, *18*, 4900.
- (20) Chichak, K. S.; Cantrill, S. J.; Pease, A. R.; Chiu, S.-H.; Cave, G. W. V.; Atwood, J. L.; Stoddart, J. F. Molecular Borromean Rings. *Science* **2004**, *304*, 1308–1312.
- (21) Lu, Y.; Deng, Y.-X.; Lin, Y.-J.; Han, Y.-F.; Weng, L.-H.; Li, Z.-H.; Jin, G.-X. Molecular Borromean Rings Based on Dihalogenated Ligands. *Chem.* **2017**, *3*, 110–121.
- (22) Sun, B.; Wang, M.; Lou, Z.; Huang, M.; Xu, C.; Li, X.; Chen, L.-J.; Yu, Y.; Davis, G. L.; Xu, B.; Yang, H.-B.; Li, X. From Ring-in-Ring to Sphere-in-Sphere: Self-Assembly of Discrete 2D and 3D Architectures with Increasing Stability. *J. Am. Chem. Soc.* **2015**, *137*, 1556–1564.
- (23) Iwamoto, T.; Slanina, Z.; Mizorogi, N.; Guo, J.; Akasaka, T.; Nagase, S.; Takaya, H.; Yasuda, N.; Kato, T.; Yamago, S. Partial Charge Transfer in the Shortest Possible Metallofullerene Peapod,  $\text{La@C}_{82}\text{C}[11]\text{Cycloparaphenylene}$ . *Chem. Eur., J.* **2014**, *20*, 14403–14409.
- (24) Ueno, H.; Nishihara, T.; Segawa, Y.; Itami, K. Cycloparaphenylene-Based Ionic Donor–Acceptor Supramolecule: Isolation and Characterization of  $\text{Li}^+\text{@C}_{60}\text{C}[10]\text{CPP}$ . *Angew. Chem., Int. Ed.* **2015**, *54*, 3707–3711.
- (25) Cogdell, R. J.; Gall, A.; Köhler, J. Q. The architecture and function of the light-harvesting apparatus of purple bacteria: from single molecules to in vivo membranes. *Rev. Biophys.* **2006**, *39*, 227–324.
- (26) Iwanaga, T.; Nakamoto, R.; Yasutake, M.; Takemura, H.; Sako, K.; Shinmyozu, T. Cyclophanes within Cyclophanes: The Synthesis of a Pyromellitic Diimide-Based Macrocycle as a Structural Unit in a Molecular Tube and Its Inclusion Phenomena. *Angew. Chem., Int. Ed.* **2006**, *45*, 3643–3647.
- (27) Zhang, Y.; Wang, H.-Q.; Zhao, Y.-Y.; Qiu, Y.-Q. New Structure-Nonlinear Optical Property Correlation in “Russian Doll” Complexes Formed by Nested Pd(II) Nanorings. *J. Phys. Chem. C* **2020**, *124* (23), 12655–12664.
- (28) Ubasart, E.; Borodin, O.; Fuertes-Espinosa, C.; Xu, Y.; García-Simón, C.; Gómez, L.; Juanhuix, J.; Gándara, F.; Imaz, I.; Maspocho, D.; von Delius, M.; Ribas, X. A three-shell supramolecular complex enables the symmetry-mismatched chemo- and regioselective bis-functionalization of  $\text{C}_{60}$ . *Nat. Chem.* **2021**, *13*, 420–427.
- (29) Grabicki, N.; Dumele, O. Confining the Inner Space of Strained Carbon Nanorings. *Synlett* **2022**, *33*, 1–7.
- (30) Jasti, R.; Bhattacharjee, J.; Neaton, J. B.; Bertozzi, C. R. Synthesis, Characterization, and Theory of [9]-, [12]-, and [18]-Cycloparaphenylene: Carbon Nanohoop Structures. *J. Am. Chem. Soc.* **2008**, *130*, 17646–17647.
- (31) Takaba, H.; Omachi, H.; Yamamoto, Y.; Bouffard, J.; Itami, K. Selective Synthesis of [12]Cycloparaphenylene. *Angew. Chem., Int. Ed.* **2009**, *48*, 6112–6116.
- (32) Yamago, S.; Watanabe, Y.; Iwamoto, T. Synthesis of [8]Cycloparaphenylene from a Square-Shaped Tetranuclear Platinum Complex. *Angew. Chem., Int. Ed.* **2010**, *49*, 757–759.
- (33) Hitosugi, S. P.; Nakanishi, W.; Yamasaki, T.; Isobe, H. Bottom-up synthesis of finite models of helical (n, m)-single-wall carbon nanotubes. *Nat. Commun.* **2011**, *2*, 492–496.
- (34) Li, K.; Xu, Z. Q.; Deng, H.; Zhou, Z. N.; Dang, Y. F.; Sun, Z. Dimeric Cycloparaphenylenes with a Rigid Aromatic Linker. *Angew. Chem., Int. Ed.* **2021**, *60*, 7649–7653.
- (35) Xu, W.; Yang, X. D.; Fan, X. B.; Wang, X.; Tung, C. H.; Wu, L. Z.; Cong, H. Synthesis and Characterization of a Pentiptycene-Derived Dual Oligoparaphenylene Nanohoop. *Angew. Chem., Int. Ed.* **2019**, *58*, 3943–3947.

- (36) (g) Xu, Y.; Kaur, R.; Wang, B.; Minameyer, M. B.; Gsänger, S.; Meyer, B.; Drewello, T.; Guldi, D. M.; von Delius, M. Concave–Convex  $\pi$ - $\pi$  Template Approach Enables the Synthesis of [10]-Cycloparaphenylene–Fullerene [2]Rotaxanes. *J. Am. Chem. Soc.* **2018**, *140*, 13413–13420.
- (37) He, J.; Yu, M.; Pang, M.; Fan, Y. Q.; Lian, Z.; Wang, Y.; Wang, W.; Liu, Y.; Jiang, H. Nanosized Carbon Macrocycles Based on a Planar Chiral Pseudo Meta-[2.2]Paracyclophane. *Chem.—Eur. J.* **2022**, *28* (13), No. e202103832.
- (38) He, J.; Yu, M.; Lian, Z.; Fan, Y.-Q.; Guo, S. Z.; Li, X.-N.; Wang, Y.; Wang, W. G.; Cheng, Z.-Y.; Jiang, H. Lemniscular carbon nanohoops with contiguous conjugation from planar chiral [2.2]-paracyclophane: influence of the regioselective synthesis on topological chirality. *Chem. Sci.* **2023**, *14*, 4426–4433.
- (39) Fan, Y. Q.; He, J.; Liu, L.; Liu, G. Q.; Guo, S. Z.; Lian, Z.; Li, X. N.; Guo, W. J.; Chen, X. B.; Wang, Y.; Jiang, H. Chiral Carbon Nanorings: Synthesis, Properties and Hierarchical Self-assembly of Chiral Ternary Complexes Featuring a Narcissistic Chiral Self-Recognition for Chiral Amines. *Angew. Chem., Int. Ed.* **2023**, *62*, No. e202304623.
- (40) Li, X. N.; Jia, L. Y.; Wang, W. G.; Wang, Y.; Sun, D.; Jiang, H. A Nonalternant azulene-embedded carbon nanohoop featuring anti-kasha emission and tunable properties upon pH stimuli-responsiveness. *J. Mater. Chem. C* **2023**, *11*, 1429.
- (41) Fan, Y.-Q.; Fan, S.; Liu, L.; Guo, S. Z.; He, J.; Li, X.-N.; Lian, Z.; Guo, W. J.; Chen, X. B.; Wang, Y.; Jiang, H. Efficient Manipulating Förster Resonance Energy Transfer through Host-Guest Interaction Enables Tunable White-Light Emission and Devices in Heterotopic Bisnanohoops. *Chem. Sci.* **2023**, *14*, 11121–11130.
- (42) Fan, Y. Q.; He, J.; Guo, S. Z.; Jiang, H. Host-Guest Chemistry in Binary and Ternary Complexes Utilizing  $\pi$ -Conjugated Carbon Nanorings. *ChemPlusChem*. **2024**, No. e202300536.
- (43) Fomine, S.; Zolotukhin, M. G.; Guadarrama, P. “Russian doll” complexes of [n]cycloparaphenylenes: a theoretical study. *J. Mol. Model.* **2012**, *18*, 4025–4032.
- (44) Bachrach, S. M.; Zayat, Z. C. “Planetary Orbit” Systems Composed of Cycloparaphenylenes. *J. Org. Chem.* **2016**, *81*, 4559–4565.
- (45) Hashimoto, S.; Iwamoto, T.; Kurachi, D.; Kayahara, E.; Yamago, S. Shortest Double-Walled Carbon Nanotubes Composed of Cycloparaphenylenes. *ChemPlusChem*. **2017**, *82*, 1015–1020.
- (46) Kawase, T.; Tanaka, K.; Shiono, N.; Seirai, Y.; Oda, M. Onion-Type Complexation Based on Carbon Nanorings and a Buckminsterfullerene. *Angew. Chem., Int. Ed.* **2004**, *43*, 1722–1724.
- (47) Kawase, T.; Nishiyama, Y.; Nakamura, T.; Ebi, T.; Matsumoto, K.; Kurata, H.; Oda, M. Cyclic [5]Paraphenyleneacetylene: Synthesis, Properties, and Formation of a Ring-in-Ring Complex Showing a Considerably Large Association Constant and Entropy Effect. *Angew. Chem., Int. Ed.* **2007**, *46*, 1086–1088.
- (48) Lu, D.; Huang, Q.; Wang, S.; Wang, J.; Huang, P.; Du, P. The Supramolecular Chemistry of Cycloparaphenylenes and Their Analogs. *Front. Chem.* **2019**, *7*, 00668.
- (49) Xu, Y.; von Delius, M. The Supramolecular Chemistry of Strained Carbon Nanohoops. *Angew. Chem., Int. Ed.* **2020**, *59*, 559–573.
- (50) Seeman, N. C. DNA in a material world. *Nature* **2003**, *421*, 427–431.
- (51) Gothelf, K. V.; LaBean, T. H. DNA-programmed assembly of nanostructures. *Org. Biomol. Chem.* **2005**, *3*, 4023–4037.
- (52) Feldkamp, U.; Niemeyer, C. M. Rationaler Entwurf von DNA-Nanoarchitekturen. *Angew. Chem.* **2006**, *118*, 1888–1910.
- (53) Saccà, B.; Meyer, R.; Feldkamp, U.; Schroeder, H.; Niemeyer, C. M. High-Throughput, Real-Time Monitoring of the Self-Assembly of DNA Nanostructures by FRET Spectroscopy. *Angew. Chem., Int. Ed.* **2008**, *47*, 2135–2137.
- (54) Förster, T. Zwischenmolekulare Energiewanderung und Fluoreszenz. *Ann. Phys.* **1948**, *437*, 55–75.
- (55) Förster, T. 10th Spiers Memorial Lecture. Transfer mechanisms of electronic excitation. *Discuss. Faraday Soc.* **1959**, *27*, 7–17.
- (56) Barrett, E. S.; Dale, T. J.; Rebek, J. Assembly and Exchange of Resorcinarene Capsules Monitored by Fluorescence Resonance Energy Transfer. *J. Am. Chem. Soc.* **2007**, *129*, 3818.
- (57) Barrett, E. S.; Dale, T. J.; Rebek, J. Self-Assembly Dynamics of a Cylindrical Capsule Monitored by Fluorescence Resonance Energy Transfer. *J. Am. Chem. Soc.* **2007**, *129*, 8818.
- (58) Barrett, E. S.; Dale, T. J.; Rebek, J. Synthesis and assembly of monofunctionalized pyrogallolarene capsules monitored by fluorescence resonance energy transfer. *Chem. Commun.* **2007**, 4224–4226.
- (59) Huang, C.-B.; Xu, L.; Zhu, J.-L.; Wang, Y.-X.; Sun, B.; Li, X. P.; Yang, H.-B. Real-Time Monitoring the Dynamics of Coordination-Driven Self-Assembly by Fluorescence-Resonance Energy Transfer. *J. Am. Chem. Soc.* **2017**, *139*, 9459–9462.
- (60) Jia, P.-P.; Xu, L.; Hu, Y.-X.; Li, W.-J.; Wang, X.-Q.; Ling, Q.-H.; Shi, X. L.; Yin, G.-Q.; Li, X. P.; Sun, H. T.; Jiang, Y. R.; Yang, H.-B. Orthogonal Self-Assembly of a Two-Step Fluorescence-Resonance Energy Transfer System with Improved Photosensitization Efficiency and Photooxidation Activity. *J. Am. Chem. Soc.* **2021**, *143*, 399–408.
- (61) Jia, P.-P.; Hu, L. R.; Dou, W.-T.; Xu, X.-D.; Sun, H. T.; Peng, Z.-Y.; Zhang, D.-Y.; Yang, H.-B.; Xu, L. An efficient hierarchical self-assembly approach to construct structurally diverse two-step sequential energy-transfer artificial light-harvesting systems. *J. Mater. Chem. C* **2023**, *11*, 6607–6615.
- (62) Teunissen, A. J. P.; Pérez-Medina, C.; Meijerink, A.; Mulder, W. J. M. Investigating supramolecular systems using Förster resonance energy transfer. *Chem. Soc. Rev.* **2018**, *47*, 7027.
- (63) Yin, J.; Hu, Y.; Yoon, J. Biosensing by luminogens with aggregation-induced emission characteristics. *Chem. Soc. Rev.* **2015**, *44* (14), 4619–4644.
- (64) Kwok, R. T.; Leung, C. W.; Lam, J. W.; Tang, B. Z. Biosensing by luminogens with aggregation-induced emission characteristics. *Chem. Soc. Rev.* **2015**, *44* (13), 4228–4238.
- (65) Wu, L.; Huang, C.; Emery, B. P.; Sedgwick, A. C.; Bull, S. D.; He, X. P.; Tian, H.; Yoon, J.; Sessler, J. L.; James, T. D. Förster resonance energy transfer (FRET)-based small-molecule sensors and imaging agents. *Chem. Soc. Rev.* **2020**, *49*, 5110–5139.
- (66) He, X. P.; Hu, X. L.; James, T. D.; Yoon, J.; Tian, H. Multiplexed photoluminescent sensors: towards improved disease diagnostics. *Chem. Soc. Rev.* **2017**, *46* (22), 6687–6696.
- (67) (a) Yang, Y.; Zhao, Q.; Feng, W.; Li, F. Luminescent Chemodosimeters for Bioimaging. *Chem. Rev.* **2013**, *113*, 192.
- (68) Cheng, H.-B.; Zhang, H.-Y.; Liu, Y. Dual-Stimulus Luminescent Lanthanide Molecular Switch Based on an Unsymmetrical Diarylperfluorocyclopentene. *J. Am. Chem. Soc.* **2013**, *135*, 10190.
- (69) Peng, H.-Q.; Sun, C.-L.; Niu, L.-Y.; Chen, Y.-Z.; Wu, L.-Z.; Tung, C.-H.; Yang, Q.-Z. Supramolecular Polymeric Fluorescent Nanoparticles Based on Quadruple Hydrogen Bonds. *Adv. Funct. Mater.* **2016**, *26*, 5483.
- (70) Teng, K. X.; Niu, L. Y.; Kang, Y. F.; Yang, Q. Z. Rational design of a “dual lock-and-key” supramolecular photosensitizer based on aromatic nucleophilic substitution for specific and enhanced photodynamic therapy. *Chem. Sci.* **2020**, *11* (35), 9703–9711.
- (71) Sun, W.; Zhao, X.; Fan, J.; Du, J.; Peng, X. Boron Dipyrromethene Nano-Photosensitizers for Anticancer Phototherapy. *Small* **2019**, *15* (32), 1804927.
- (72) Peng, H.-Q.; Niu, L.-Y.; Chen, Y.-Z.; Wu, L.-Z.; Tung, C.-H.; Yang, Q.-Z. Biological Applications of Supramolecular Assemblies Designed for Excitation Energy Transfer. *Chem. Rev.* **2015**, *115*, 7502.
- (73) Guo, S.; Song, Y.; He, Y.; Hu, X. Y.; Wang, L. Highly Efficient Artificial Light-Harvesting Systems Constructed in Aqueous Solution Based on Supramolecular Self-Assembly. *Angew. Chem., Int. Ed.* **2018**, *57* (12), 3163–3167.
- (74) Lian, Z.; He, J.; Liu, L.; Fan, Y. Q.; Chen, X. B.; Jiang, H. [2,2] Paracyclophanes-based double helicates for constructing artificial light-harvesting systems and white LED device. *Nat. Commun.* **2023**, *14*, 2752.
- (75) Zhang, D. Q.; Li, M.; Jiang, B.; Liu, S. K.; Yang, J.; Yang, X.; Ma, K.; Yuan, X. J.; Yi, T. Three-step cascaded artificial light-



harvesting systems with tunable efficiency based on metallocycles. *J. Colloid Interface Sci.* **2023**, *652*, 1494–1502.

(76) Guo, S. Z.; Liu, L.; Li, X. N.; Liu, G. Q.; Fan, Y. Q.; He, J.; Lian, Z.; Yang, H. J.; Chen, X. B.; Jiang, H. Highly Luminescent Chiral Carbon Nanohoops via Symmetry Breaking with a Triptycene unit: Bright Circularly Polarized Luminescence and Size-dependent Properties. *Small* **2023**, 2308429.

(77) Ogoshi, T.; Kanai, S.; Fujinami, S.; Yamagishi, T.-a.; Nakamoto, Y. para-Bridged Symmetrical Pillar[5]arenes: Their Lewis Acid Catalyzed Synthesis and Host–Guest Property. *J. Am. Chem. Soc.* **2008**, *130*, 5022–5023.

(78) Xue, M.; Yang, Y.; Chi, X.; Zhang, Z.; Huang, F. Pillararenes, A New Class of Macrocycles for Supramolecular Chemistry. *Acc. Chem. Res.* **2012**, *45*, 1294–1308.

(79) Liu, X.; Weinert, Z. J.; Sharafi, M.; Liao, C.; Li, J.; Schneebeli, S. T. Regulating Molecular Recognition with C-Shaped Strips Attained by Chirality-Assisted Synthesis. *Angew. Chem. Int. Ed.* **2015**, *54*, 12772–12776.

(80) Ogoshi, T.; Yamagishi, T.-a.; Nakamoto, Y. Pillar-Shaped Macrocyclic Hosts Pillar[n]arenes: New Key Players for Supramolecular Chemistry. *Chem. Rev.* **2016**, *116*, 7937–8002.

(81) Wang, Y.; Ping, G.; Li, C. Efficient complexation between pillar[5]arenes and neutral guests: from host–guest chemistry to functional materials. *Chem. Commun.* **2016**, *52*, 9858–9872.

(82) Wu, J.-R.; Wu, G.; Li, D.; Yang, Y.-W. Macrocyclic-Based Crystalline Supramolecular Assemblies Built with Intermolecular Charge-Transfer Interactions. *Angew. Chem., Int. Ed.* **2023**, *62*, No. e20221814.

(83) Zeng, F.; Tang, L. L.; Ding, M. H.; Dessie, W. Giant Cavity Macrocyclic: Synthesis, Structure, and Its Complexation with Pagoda[5]arene. *Org. Lett.* **2023**, *25*, 6290–6294.

(84) Lefebvre, C.; Rubez, G.; Khartabil, H.; Boisson, J. C.; Contreras-García, J.; Hénon, E. Accurately extracting the signature of intermolecular interactions present in the NCI plot of the reduced density gradient versus electron density. *Phys. Chem. Chem. Phys.* **2017**, *19*, 17928–17936.

(85) Huang, T. -T.; Chen, J. -F.; Liu, J.; Wei, T. -B.; Yao, H.; Shi, B. B.; Lin, Q. A novel fused bi-macrocyclic host for sensitive detection of Cr<sub>2</sub>O<sub>7</sub><sup>2-</sup> based on enrichment effect. *Chinese Chem. Lett.* **2023**, 109281.